Journal of
Marine Science and Engineering

MDPI

Article

Optimization of the Number, Hub Height and Layout of Offshore Wind Turbines

Haiying Sun [1,*], Hongxing Yang [2,*] and Siyu Tao [3]

[1] School of Marine Science and Engineering, South China University of Technology, Guangzhou 511400, China
[2] Renewable Energy Research Group, Department of Building Environment and Energy Engineering, The Hong Kong Polytechnic University, Hong Kong 999077, China
[3] College of Automation Engineering, Nanjing University of Aeronautics and Astronautics, Nanjing 211106, China
* Correspondence: sunhaiying@scut.edu.cn or haiying.sun@connect.polyu.hk (H.S.); hong-xing.yang@polyu.edu.hk (H.Y.)

Abstract: In order to make full use of the potential of wind resources in a specific offshore area, this paper proposes a new method to simultaneously optimize the number, hub height and layout of a wind farm. The wind farm is subdivided by grids, and the intersection points are set as the potential wind turbine positions. The method adopts a genetic algorithm and encodes wind farm parameters into chromosomes in binary form. The length of chromosomes is decided by the number of potential positions and the hub heights to be selected. The optimization process includes selection, crossover, and mutation, while the efficiency of wind farm is set as the optimization objective. The proposed method is validated by three benchmark cases. It has proven to be effective in deciding the number of turbines and improving the efficiency of the wind farm. Another advantage of the proposed method is that it can be widely applied to wind farms of any shape. A case study applying the new method to an irregularly shaped wind farm in Hong Kong is demonstrated. By comparing the results with the original regularly shaped wind farm, the new method can improve power generation by 6.28%. Therefore, the proposed model is a supportive tool for designing the best number, hub heights and positions of wind turbines.

Keywords: wind turbine number; hub height; genetic algorithm; wake effect; offshore wind farm layout optimization

Citation: Sun, H.; Yang, H.; Tao, S. Optimization of the Number, Hub Height and Layout of Offshore Wind Turbines. *J. Mar. Sci. Eng.* **2023**, *11*, 1566. https://doi.org/10.3390/jmse11081566

Academic Editors: Unai Fernandez-Gamiz and Dong-Sheng Jeng

Received: 3 July 2023
Revised: 21 July 2023
Accepted: 3 August 2023
Published: 9 August 2023

1. Introduction

Wind energy is a well-known renewable energy. As a result of its inexhaustible and clean characteristics [1], wind energy is becoming significant all around the world [2]. For a wind farm, many impactors will influence the economic performance, such as the type of wind turbine, foundation, and installation cost, etc. [3] The number of wind turbines is critical, as it will directly affect the total capacity and the efficiency. It is easy to understand that more wind turbines can increase the energy capacity, however, due to the wake effect, wind losses will become serious where wind turbines are installed close to each other. Therefore, a good balance between the capacity and energy loss should be carefully considered when selecting the wind turbine number.

The possible layouts of a wind farm can be countless. To make wind farm design and optimization simple, the gird-based method is commonly used. It subdivides the wind farm into small square parts, of which each grid represents a possible position for a wind turbine. Representative studies includes references [4–15], taking the centers of squares as the potential positions, and reference [16], taking the intersection points as the potential positions. Even under this circumstance, the possible wind turbine layouts are numerous. The computational cost for calculating all layouts is quite large. The wind farm under study is considered to have N_P potential positions for wind turbines, and N_{WT} wind turbines, thus the total number of distinct solutions is given as Equation (1).

$$N_{Sol} = C_{N_P}^{N_{WT}} = \frac{N_P!}{N_{WT}!(N_P - N_{WT})!} \quad (1)$$

If the number of turbines is not determined, the number of possible distinct solutions is even more, as given as (2).

$$N_{Sol} = 2^{N_p} \quad (2)$$

The large number of possibilities results in a huge computational cost. In addition, the aforementioned equations are based on the assumption that a wind farm has a fixed number of available positions. The shortcoming of this is that the wind turbines can be installed only on the available locations, and the layout patterns involving wind turbines installed on other points are ignored [17]. If turbines can be constructed at any position on the wind farm then the number of possible layouts will increase, and the computational cost for layout optimization will increase dramatically as well.

Optimizing positions of wind turbines is a complex problem. Even in one dimension, it has no analytical solution [18]. In many studies, N_{WT} is assumed to be known before constructing a wind farm [19]. This makes designing a wind farm relatively easy, when compared to a situation wherein both the number and turbine locations have to be determined [20]. Pérez et al. [21] applied a heuristic method and nonlinear techniques to improve offshore wind farms' power output. Rodrigues et al. [22] presented an optimization framework for a wind farm containing moveable floating wind turbines, which can simultaneously optimize the anchoring location and the wind turbine position. Hou et al. [23] proposed a restriction zone concept and integrated it into an offshore wind farm optimization method. Gebraad et al. [24] used wake steering based on yaw control with layout changes to maximize the wind plant annual energy production. The combined method can increase the annual energy production by 5%. Kirchner-Bossi and Porte-Agel [25] integrated a Gaussian wake model with an evolutionary wind farm layout optimization methodology, which can both attain greater power generation and decrease the electricity cable length among turbines. Song et al. [26] used Gaussian Particle Swarm Optimization to determine patterns of wind turbines with multiple heights installed on flat terrain. Reddy [27] developed a method considering the elevation of terrain and the profile of ambient wind. Moreno et al. [28] developed a multi-objective algorithm for designing layout of a wind farm, the objectives of which included decreasing energy cost, wind farm area and wake-induced loss.

The aforementioned methods to select the wind turbine positions assume that the number of turbines within the wind farm is known. However, simply assuming a N_{WT} may not obtain the optimal results. Moreover, in engineering, the wind farm designers usually have little knowledge about the best number of wind turbines to construct [17]. Therefore, an investigation of best number of turbines is necessary. Mustakerov and Borissova [29] developed an approach for choosing wind turbine type, number and position based on the given environment conditions and wind farm area. In the proposed method, the optimization problem was regarded as a combinatorial task of a single criterion and a mixed-integer nonlinear discrete criterion. Ekonomou et al. [30] presented an Artificial Neural Network method that can decide the best quantity of wind turbines and energy generation of a wind farm. Feng et al. [31] presented a multi-objective algorithm that could simultaneously optimize the number and position of wind turbines. The method formulated the positions of wind turbines as continuous variables. In addition, two objectives were considered, including increasing the power generation and decreasing the length of electrical cable. Mittal et al. [17] proposed an optimization methodology combining the probabilistic genetic algorithms and deterministic gradient methods, which can optimize the number of turbines as well as the turbine positions on the wind farm.

Mittal et al. [32] optimized the number and positions of turbines by balancing energy and noise.

All of these studies help to decide on the number of turbines on a uniform wind farm, where all turbines are of a same type. Recent studies have shown that a wind farm consisting of turbines with different hub heights may have a larger power efficiency [33]. However, the question of how to decide on the number of turbines at different hub heights has not been investigated in depth. Therefore, this research proposes a novel binary method to simultaneously optimize the number, hub heights and layout of wind turbines. The rest of this paper is structured as follows. In Section 2, the proposed method is introduced in detail, including models for simulating wind farm performance and the optimization algorithm. In Section 3, the effectiveness of the new methodology is evaluated by conducting three typical case studies and comparing them with the benchmark results. In Section 4, the impact of hub height on wind farm efficiency is discussed, and a series of hub height differences from 5 m to 50 m are included. In Section 5, the procedure of applying the proposed method to irregularly shaped wind farms is described and an application on an offshore wind farm in Hong Kong is demonstrated. Finally, the major conclusions drawn from this paper are summarized in Section 6. Based on this research, the proposed binary method is effective to simultaneously decide on the number and hub heights of wind turbines on a non-uniform wind farm.

2. Model Setting

Mosetti et al. [34] first investigated the wind turbine number and layout optimization problem on a square wind farm. Three cases were demonstrated, which are regarded as benchmark by the following scholars. Therefore, to assess the validity of the presented method, results from the new method are compared with those benchmark results.

2.1. Wind Farm Model

The wind farm is square-shaped and its size is 20 km × 20 km. The minimum spacing between wind turbines is restricted to 5D (D represents wind turbine's rotor diameter).

2.1.1. Potential Positions

The wind farm is subdivided into several equal square cells. The wind farm has 10 × 10 grids. In the study by Mosetti et al. [34], each cell center is a potential location for wind turbines, and therefore 100 potential positions were contained in the optimization. In this study, each intersection point is a possible location, therefore there are 121 potential positions. Figure 1 demonstrates the potential positions for wind turbines in the two studies.

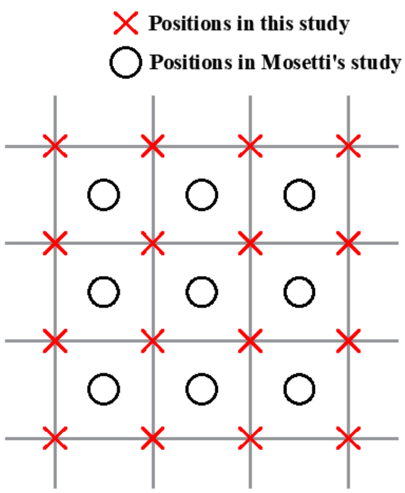

Figure 1. Potential positions for wind turbines.

2.1.2. Wind Turbine

Only one type of wind turbine is applied in this paper, of which the parameters are shown in Table 1. The size of the wind farm is 50D × 50D. Compared to 100 possible turbine locations in the original study [34], there are 121 possible turbine locations in this study.

Table 1. Parameters of wind turbine.

Parameter	Value
Hub Height ($h0$)	60 m
Rotor Diameter (D)	40 m
Thrust Coefficient (Ct)	0.88
Roughness ($z0$)	0.3 m
Rated Wind Speed (u_R)	12.8 m/s
Cut-Out Wind Speed (u_{CO})	18 m/s
Rated Power (P_R)	630 kW

The function for the wind turbine's power curve is as follows.

$$P = \begin{cases} 0.3u^3, & 0 \leq u \leq u_R \\ P_R & u_R < u \leq u_{CO} \\ 0, & u > u_{CO} \end{cases} \tag{3}$$

2.1.3. Wake Effect

The wake effect happens behind operating wind turbines and continues for a long distance, which has a negative influence on the downwind wind turbines [35]. The Jensen wake model is widely used, but its assumptions are unrealistic. To be specific, wind speed is assumed to be constant at a specific downwind distance and the same at different radial positions [36]. To overcome these shortcomings, an improved two-dimensional Jensen wake model is adopted in this paper [37]. In this wake model, the wake influence on the downstream turbine has a close relationship with the relative position between the two wind turbines. Considering the hub height difference and relative position between the two turbines, the wake-influenced area is explained in Figure 2.

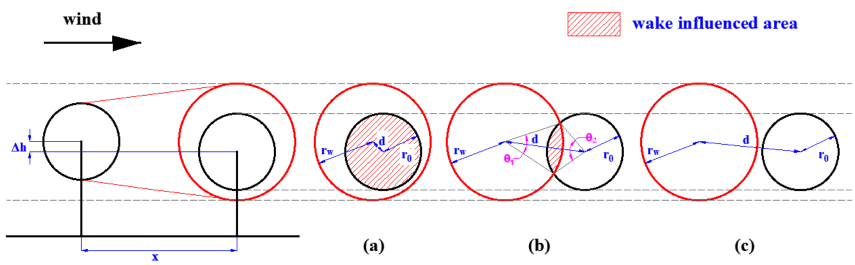

Figure 2. Wake-influenced area.

x is the downwind distance between two turbines. Δh is the difference in hub height. r_0 is the radius of the rotor. r_w is the radius of the circular wake-affected area. d is the spacing between wind turbines projected in the direction perpendicular to the inflow. The wake-influenced area for the downwind turbine has three situations [38]. In Figure 2a, where $d < r_w - r$, the downwind turbine is totally affected by wakes. In Figure 2b, where $r_w - r_0 \leq d \leq r_w + r_0$, only part of the downwind turbine is influenced by the wake effect. In Figure 2c, where $r_w + r_0 < d$, the downwind turbine is under no wake effect. Assuming

S to be the downstream turbine's swept area and S_w to be the area influenced by wakes, they can be calculated by Equations (4) and (5).

$$S = \pi {r_w}^2 \tag{4}$$

$$S_w = \frac{\theta_1 {r_w}^2}{2} + \frac{\theta_2 {r_0}^2}{2} - r_w d \sin\frac{\theta_1}{2} \tag{5}$$

θ_1 and θ_2 are two angles demonstrated in Figure 2b, which can be calculated by Equations (6) and (7), respectively.

$$\theta_1 = 2\mathrm{arccos}\frac{{r_w}^2 + d^2 - {r_0}^2}{2 r_w d} \tag{6}$$

$$\theta_2 = 2\mathrm{arccos}\frac{{r_0}^2 + d^2 - {r_w}^2}{2 r_0 d} \tag{7}$$

Assuming u_0 is the incoming wind speed, Equation (8) shows the calculation of the wind speed of the downstream turbine.

$$\begin{cases} u = u_0\left[1 - \frac{2ar_0^2}{(r_0+\alpha x)^2}\right], & d < r_w - r_0 \\ u = u_0\left[1 - \frac{2ar_0^2}{(r_0+\alpha x)^2} \cdot \frac{S_w}{S}\right], & r_w - r_0 \le d \le r_w + r_0 \\ u = u_0, & r_w + r_0 < d \end{cases} \tag{8}$$

2.1.4. Cost

To consider the cost's influence on number of wind turbines, a non-dimensionalized cost/year is adopted. Specifically, the wind turbine's annual cost is regarded as 1. The greatest cost reduction is assumed to be 1/3, which happens to a wind turbine when it is surrounded by plenty of other turbines. Referring to the study of Mosetti et al. [34], the total annual cost of wind farm is shown in Equation (9).

$$Cost_T = N_{WT}(\frac{2}{3} + \frac{1}{3}e^{-0.00174{N_{WT}}^2}) \tag{9}$$

2.2. Optimization Algorithm

A genetic algorithm (GA) has proven to be an effective tool for optimizing positions of wind turbines [39], and is therefore is adopted in this study. The information of number, hub heights and layout are all involved in the chromosome. The structure of the chromosome is demonstrated in Figure 3.

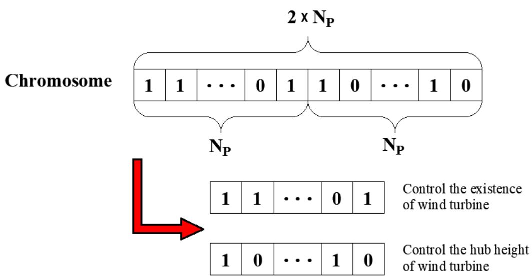

Figure 3. The chromosome of GA in this study.

The number and hub height of turbine are simultaneously optimized to obtain an optimal result. To be specific, for N_P potential positions, each chromosome has $2N_P$ binary numbers. The first N_P numbers represent the existence of wind turbines. If the number is 1, the corresponding position has a wind turbine, while if the number is 0, the corresponding position has no wind turbine. The second N_P numbers represent the hub height information. Two hub heights are involved in this study, and 1 and 0 represent the two different hub heights, respectively. For example, when the hub heights of h_1 and h_2 are considered, if the binary number is 1, then the corresponding hub height is h_1, while if the binary number is 0, the corresponding hub height is h_2. If more hub heights are considered on a wind farm, they should be controlled with the corresponding binary numbers. Thus, different configurations of wind farm could be represented by the chromosome.

The optimization objective is to achieve the most energy generation at a certain cost. Assuming P_T is the power output per year, the function of the objective is as follows.

$$Objective = \frac{P_T}{Cost_T} \tag{10}$$

The procedure of the proposed method for the wind farm optimization problem is demonstrated in Figure 4. As mentioned before, 5D is set as the restriction distance in this paper, but other restriction distances can also be applied according to the actual working conditions. Next, the grid of potential positions based on the restriction distance will be applied to the wind farm, and all potential positions for wind turbines are determined. Then, the potential positions should be numbered for coding the chromosome and then for optimizing the layout. The information on wind turbine existence and hub height will be simultaneously coded in one chromosome. The number of hub height options will influence the length of chromosome. After the process of configuring the wind farm, the work of initialization for GA optimization can be conducted. Each chromosome represents a unique wind farm design, and the annual energy production can be calculated by considering the wind turbine number and the wake-induced power loss. All chromosomes will be judged by the elitist strategy and sorted according to the fitness evaluation [40]. When the termination condition is met, the optimized result is obtained. Otherwise, the chromosomes will go into the selection, crossover and mutation processes, and new results will be generated. In the selection part, the fittest individuals are selected and generated. In the crossover part, features of good surviving individuals are propagated into the next population. The mutation process promotes diversity in population. This process will repeat until the termination criterion is met, and the optimized result will be obtained in the end.

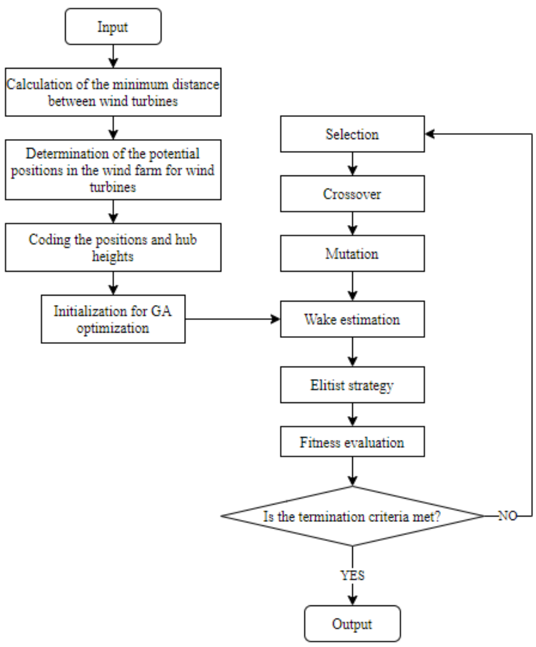

Figure 4. Process demonstration of the methodology.

The setting of parameters for the GA process used in this research is shown in Table 2.

Table 2. The parameter setting for GA.

Parameter	Value
Individual Size	200
Mutation Probability	0.01–0.1
Crossover Probability	0.6–0.9
Iteration	400

3. Benchmark Case Study—Two Hub Heights

The hub height in the benchmark study is 60 m. To evaluate the validity of the new method, two hub heights of 55 m and 65 m are adopted in this study. Three case studies with different incoming wind conditions are conducted to evaluate the proposed optimization method. The cases include: (1) a single wind direction; (2) multiple wind directions with a constant intensity; and (3) multiple wind directions and intensities.

3.1. Case 1—A Single Wind Direction

The wind speed in Case 1 is set to be constant. The incoming wind is 12 m/s. The wind comes from north, i.e., wind direction is 0°. The wind distribution for this case is demonstrated in Figure 5. Figure 6 demonstrates the optimized layout and hub heights of wind turbines in Case 1 and compares them with the original result.

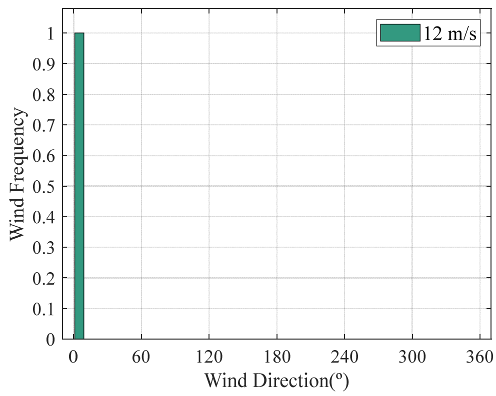

Figure 5. Wind distribution for the Case 1: a constant intensity and a single direction.

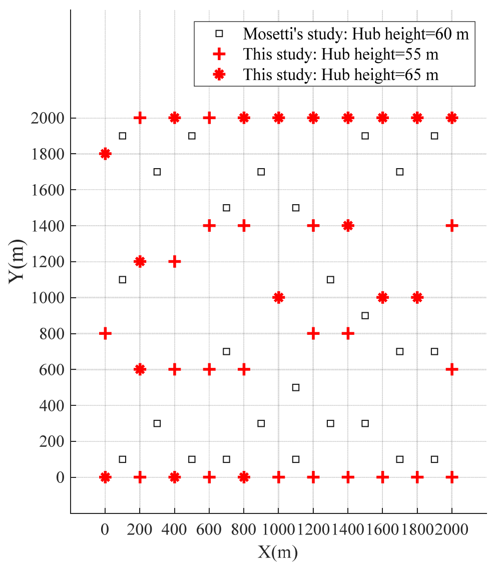

Figure 6. Optimized results of Case 1.

Table 3 compares the results from this study with those from Mosetti's study. The optimized turbine number in Mosetti's study is 25, while the number in this study is 40, among which 18 are 55 m high and 22 are 65 m high. The annual non-dimensionalized cost reduces from 1.57×10^{-3} to 1.43×10^{-3}. The wind farm's efficiency shows a little reduction, from 0.95 to 0.93, but the annual total power increases from 12,375 kW to 19,222 kW. Therefore, in this case, the proposed method both improves the power output and reduces the cost.

Table 3. Optimized parameters of this study compared with Mosetti's study for Case 1.

	Efficiency of Wind Farm	Annual Total Power (kW)	Annual Non-Dimensionalized Cost	Number of Turbines
Mosetti's Study	0.95	12,375	1.57×10^{-3}	25 (Hub height: 60 m)
This Study	0.93	19,222	1.43×10^{-3}	18 (Hub height: 55 m) 22 (Hub height: 65 m)

3.2. Case 2—Multiple Wind Directions with a Constant Intensity

In this case, the incoming wind speed is set as 12 m/s, but the wind blows evenly from all 360° directions. The wind distribution for this case is demonstrated in Figure 7. Figure 8 demonstrates the optimized layout and hub heights of wind turbines in Case 2, and the results are also compared with the original study.

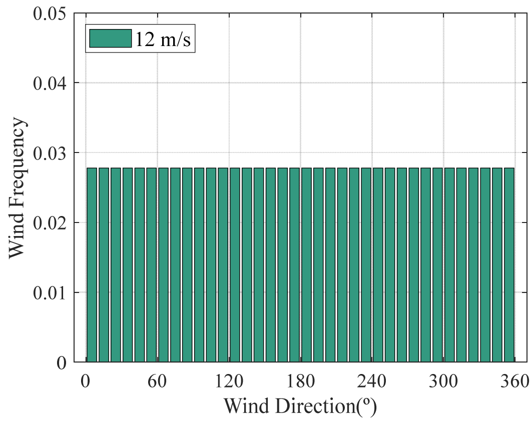

Figure 7. Wind distribution for Case 2: a constant intensity and variable directions.

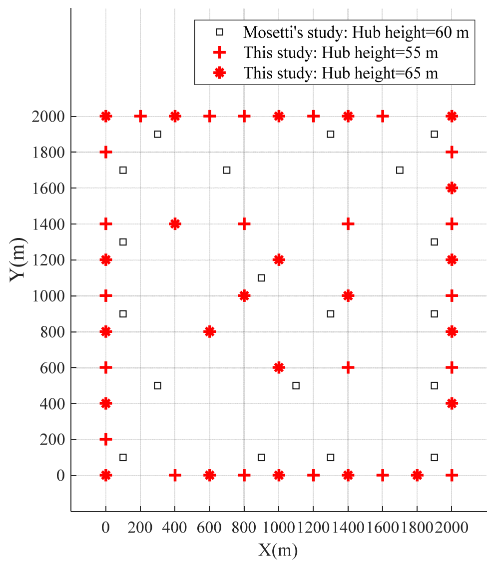

Figure 8. Optimized layouts of Case 2.

Table 4 compares the results from this study with those from Mosetti's study. The optimized number of wind turbines in Mosetti's study is 19, while it is 45 in this study. A total of 22 wind turbines are at the 55 m hub height and 23 are at the 65 m hub height. The annual non-dimensionalized cost reduces from 1.84×10^{-3} to 1.44×10^{-3}. The efficiency of the wind farm increases from 0.88 to 0.91. The annual power also increases, from 8711 kW to 21,168 kW. In this case, the proposed method significantly improves the wind farm's performance in all aspects involved. In particular, the annual total power is about 2.5 times the original results.

Table 4. Optimized parameters of this study compared with Mosetti's study for Case 2.

	Efficiency of Wind Farm	Annual Total Power (kW)	Annual Non-Dimensionalized Cost	Number of Turbines
Mosetti's Study	0.88	8711	1.84×10^{-3}	19 (Hub height: 60 m)
This Study	0.91	21,168	1.44×10^{-3}	22 (Hub height: 55 m) 23 (Hub height: 65 m)

3.3. Case 3—Multiple Wind Directions and Intensities

In Case 3, the wind speed is not a constant, and the wind direction changes as well. The wind distribution for this case is shown in Figure 9. Figure 10 demonstrates the optimized layout and hub heights of wind turbines in Case 3, which are compared with the original result.

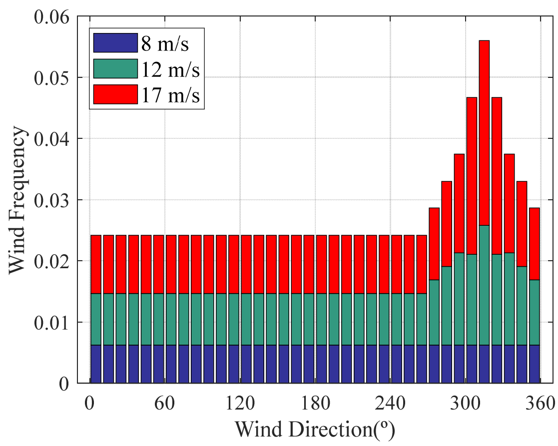

Figure 9. Wind distribution for the Case 3: variable intensities and variable directions.

Table 5 compares the results of this case. In Mosetti's study, the optimized turbine number is 15, and that in this study is 51. A total of 26 turbines are 55 m high and the other 25 are 65 m high. The annual non-dimensionalized cost reduces from 3.61×10^{-3} to 1.45×10^{-3}. The efficiency of the wind farm increases from 0.84 to 0.95, and the annual power also increases from 3695 kW to 23,514 kW. In this case, the proposed method also significantly improves the efficiency and power generation performances of the wind farm.

Table 5. Optimized parameters of this study compared with Mosetti's study for Case 3.

	Efficiency of Wind Farm	Annual Total Power (kW)	Annual Non-Dimensionalized Cost	Number of Turbines
Mosetti's Study	0.84	3695	3.61×10^{-3}	15 (Hub height: 60 m)
This Study	0.95	23,514	1.45×10^{-3}	26 (Hub height: 55 m) 25 (Hub height: 65 m)

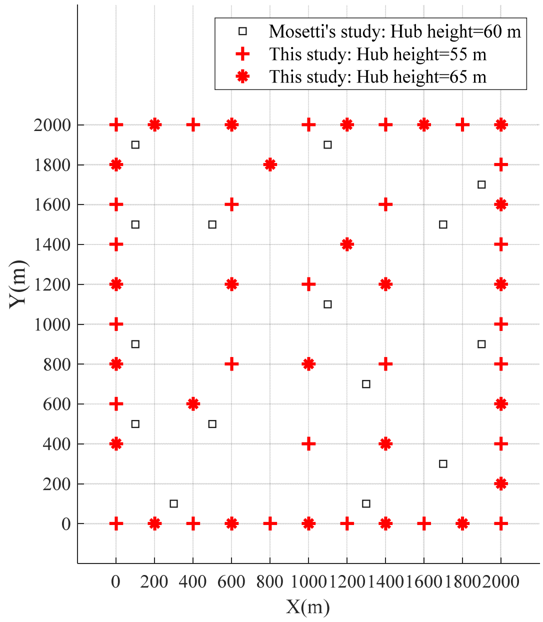

Figure 10. Optimized layouts of Case 3.

Based on the aforementioned three case studies, the proposed method is helpful for improving the performance of wind farm. Adopting two hub heights can significantly reduce the annual non-dimensionalized cost. In all cases, if the proposed method is adopted, more turbines could be constructed within a wind farm. This also results in an important improvement in annual energy output. The wind farm's efficiency has different performance in three cases, but all three efficiencies are acceptable as they are larger than 0.91.

4. The Impact of Hub Height on Wind Farm Efficiency

To investigate the impact of hub height on efficiency of a wind farm, a series of hub height differences are adopted. The wind farm optimization is conducted under different hub height differences. The wind condition of Case 3 is applied, and the wind farm efficiency is shown Figure 11.

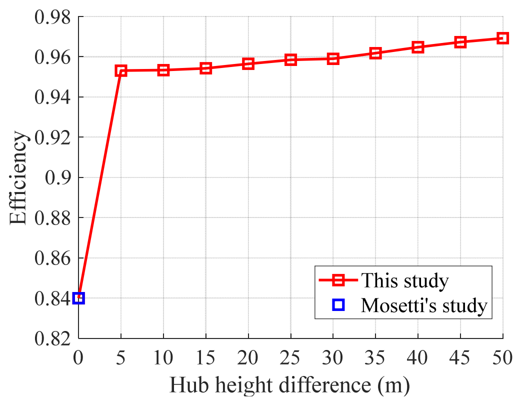

Figure 11. Efficiency of wind farm under different hub height differences.

The range of hub height difference is between 5 m and 50 m. With the hub height difference increasing, the efficiency of the wind farm also has a significant increasing trend. When difference of hub height is 5 m, the efficiency of wind farm is 0.952. If the hub height difference increases by 50 m, the efficiency will increase to 0.970. Mosetti's study contained identical turbines and the wind farm efficiency was only 0.84. If wind turbines are at the same height, wind farm optimization can only be conducted in the horizontal plan to avoid the impact from wakes. If wind turbines have two or more hub height options, the optimization is not limited to the horizontal plane; the vertical direction should also be considered. Therefore, adopting wind turbines of different hub heights contributes to improving the efficiency of wind farm.

5. Application for Irregularly Shaped Wind Farms

The proposed binary wind farm optimization method can be applied to both the regularly shaped wind farms and the irregularly shaped wind farms. The application on the regularly shaped wind farms has been demonstrated in the aforementioned study. The application on irregularly shaped wind farms will be demonstrated in this section. The method will also be adopted for the design of an offshore wind farm for Hong Kong based on the actual wind data.

5.1. Deciding Potential Wind Turbine Locations

In an irregularly shaped wind farm, the major difference from the regularly shaped wind farm lies in coding the potential positions. The entire wind farm area should be firstly subdivided into grids according to the distance restriction. Then, the length of each chromosome can be decided based on numbers of intersections and hub height options. Each number in the chromosome corresponds to the existence and hub height information of wind turbines. When estimating the wake effect, the related positions among wind turbines should be calculated according to the actual location on the irregularly shaped wind farm.

5.2. A Case Study

Hong Kong covers a total area of 2755 km^2, including 1107 km^2 land area and 1648 km^2 water area [41]. It has great advantages for exploiting offshore wind energy. Sun et al. [42] discussed the offshore wind energy with regards to a repowering strategy in the seawater area around Sha Chau Island. Gao et al. [6] conducted a feasibility study on developing wind power in Hong Kong. They show that the Waglan Island sea area has huge offshore wind energy potential. Figure 12 demonstrates the wind conditions in the Waglan Island sea area.

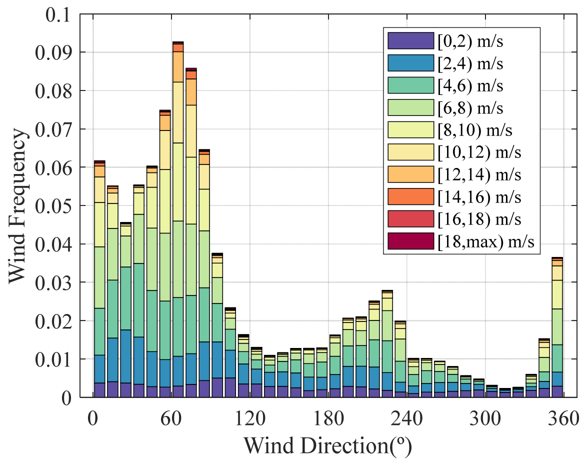

Figure 12. Wind distribution in Waglan Island sea area.

The Waglan sea area is an ideal area for wind energy, in which most wind speeds are between 6 and 12 m/s. It is also the largest one among all suitable sea areas, and is therefore selected in this research. For the area, a rectangular area is selected by Gao et al. [6] The area has a size of 3740 m × 5828 m, which is shown in the pink area in Figure 13. However, it is clear that due to the restriction of the rectangular shape, plenty of the area cannot be made good use of. Therefore, in this study, a new irregularly shaped offshore wind farm is proposed in the Waglan sea area. The shape and size are also demonstrated in Figure 13.

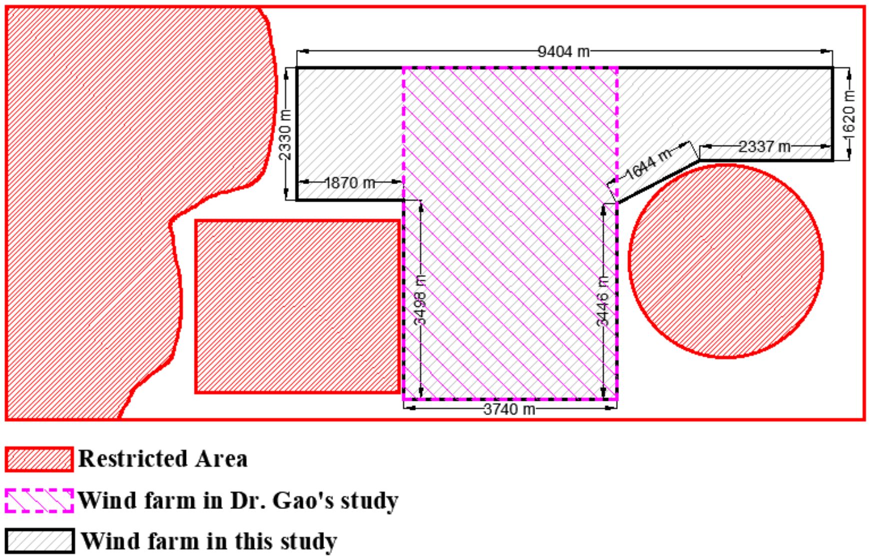

Figure 13. Proposed wind farm near Waglan Island.

The area of the original regularly shaped wind farm is 21.80 km^2, while that of the new irregularly shaped wind farm is 32.86 km^2. The wind turbine model is the same as that in Section 2.1. The restriction distance is set as 5D, which is 200 m in this case. As introduced previously, the wind farm should be subdivided into small grids based on the restriction distance. Figure 14 demonstrates the subdivided grids of two wind farms. The intersection points of these square grids are the potential locations of wind turbines.

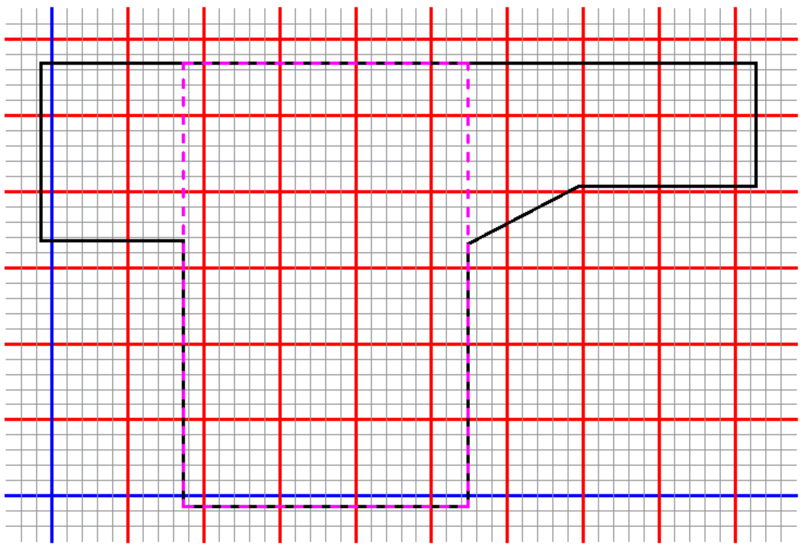

Figure 14. Grids of wind farms.

From Figure 14, the original regularly shaped wind farm has 551 intersection points, which means there are 551 potential locations. By contrast, the new wind farm has 827 intersection points. It has more potential locations for wind turbines, indicating a greater energy capacity than the original one. Two hub heights of 50 m and 70 m are applied in the optimization. The variation of wind speed in the vertical direction is considered in this study. The power law is applied, and the equation is as follows [42]:

$$v = v_0 \cdot \left(\frac{z}{z_0}\right)^{\alpha} \tag{11}$$

In the equation, z_0 is a reference height; v_0 is the wind speed at z_0; v is the wind speed at the height of z and α is the empirically derived power law coefficient that varies dependent upon the stability of the atmosphere. When the wind blows through a considerable distance from smooth terrain to rough terrain, the variation can be described by Equation (12). V_g is the gradient wind velocity that remains unchanged:

$$V_1 = V_g \cdot \left(\frac{z_1}{\delta_1}\right)^{\alpha_1}, \quad V_2 = V_g \cdot \left(\frac{z_2}{\delta_2}\right)^{\alpha_2} \tag{12}$$

Consequently, the following equation can be obtained:

$$\frac{V_2}{V_1} = \left(\frac{z_2}{\delta_2}\right)^{\alpha_2} \cdot \left(\frac{\delta_1}{z_1}\right)^{\alpha_1} \tag{13}$$

The chromosome in the regularly shaped case has 1102 binary number codes, and the chromosome in the irregularly shaped case has 1654 binary number codes. In Figure 14, blue lines are the coordinate axes and each potential location has its relative coordinates for the optimization process. During the optimization, the existence of a turbine and hub height at each potential position are decided simultaneously. The optimized results of two potential wind farms are demonstrated in Figure 15.

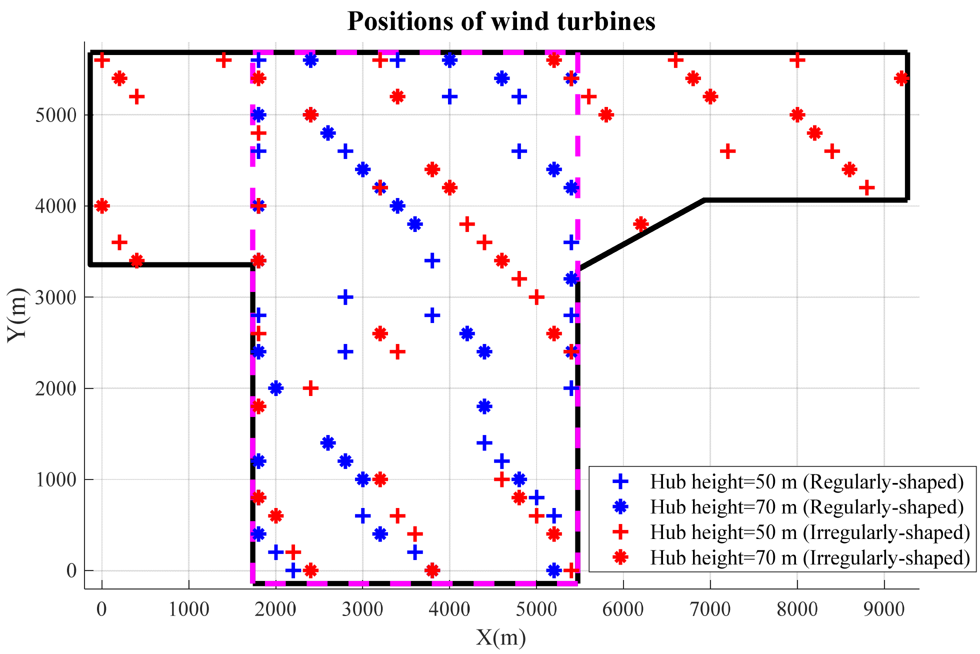

Figure 15. Comparison of optimization results.

In Figure 15, the blue points represent wind turbines optimized for the original regularly shaped wind farm, and the red points represent wind turbines optimized for the new irregularly shaped wind farm. Comparing the two layouts, the new wind farm has more space for wind turbines and the interval is also larger. The layouts are highly correlated with wind direction. From Figure 12, the prevailing wind is from northeast. Therefore, the northeast intervals are relatively larger than the crosswind ones. Optimized parameters of these two layout strategies are shown in Table 6. The annual non-dimensionalized cost is still the objective of the two optimization processes. The values of the two strategies are very close, and the efficiencies are all larger than 0.98. The optimized regularly shaped wind farm has 55 wind turbines, of which 31 are 50 m high and the other 24 are 70 m high. On the optimized irregularly shaped wind farm, there are 58 wind turbines, those of 50 m and those of 70 m each account for half. The difference in the turbine number results in the difference in the total power of two wind farms. The regularly shaped wind turbine farm has an annual total power of 5658.0 kW, and the new irregularly shaped wind turbine farm has an annual total power of 6013.1 kW. Increasing the area of the wind field improves the power. In this case, a 6.28% improvement in the total power can be achieved by making use of the additional area of the wind farm.

Table 6. Optimized parameters of two strategies.

	Efficiency of Wind Farm	Annual Total Power (kW)	Annual Non-Dimensionalized Cost	Number of Turbines
Regularly Shaped	0.981	5658.0	6.4976×10^{-3}	31 (Hub height: 50 m) 24 (Hub height: 70 m)
Irregularly Shaped	0.988	6013.1	6.4396×10^{-3}	29 (Hub height: 50 m) 29 (Hub height: 70 m)

6. Conclusions

This paper proposed a binary method for investigating the wind farm layout optimization problem by simultaneously considering the number and hub heights of wind turbines. Major conclusions drawn from this study are summarized as follows.

(1) A new wind farm optimization method is proposed wherein the number and hub heights of wind turbines could be optimized simultaneously. The newly proposed method subdivides wind farms into square grids based on the restriction distance and sets the interaction points for potential positions of wind turbines. A genetic algorithm (GA) is adopted as the optimization method. The chromosome consists of binary numbers that represent all wind turbines' positions and hub heights.

(2) The method is evaluated by comparing the results with three benchmark studies. The wake effect caused by the hub height difference is considered by applying a two-dimensional wake model. The results show that when the hub height difference is 10 m, this method can increase the annual power generation under all wind conditions and can significantly reduce the annual non-dimensionalized cost.

(3) The proposed method can also improve the power efficiency of the entire wind farm. The influence of hub height on efficiency is studied with height difference ranges from 5 m to 50 m. It is found that applying wind turbines with different heights can profoundly increase the wind farm's efficiency. To be specific, the efficiency increases from 0.952 to 0.970 when the hub height difference increases from 5 m to 50 m.

(4) The proposed method is also effective for optimizing irregularly shaped wind farms. By subdividing the wind farm with square grids with the restriction distance, all potential wind turbine positions can be obtained and then optimized by GA. An application in the offshore area around Waglan Island is shown and compared with a regularly shaped wind farm in this area. The new method improves the wind farm capacity by 6.28%, which provides an important strategy for offshore wind power development in Hong Kong.

The newly proposed methodology for wind farm optimization fills the research gap of simultaneously deciding the number and hub heights of wind turbines. According to the case study, this method can significantly improve an offshore wind farm's capacity and power efficiency. Notably, there are still some limitations need to be solved. The potential wind turbine positions are decided by square grids, of which the side length is the restriction distance. However, this is a simplified method and may exclude the actual best layout because the positions of the best layout may be continuous rather than based on a grid. Therefore, further studies should be conducted to look for better layouts based on continuous coordinates.

Author Contributions: Conceptualization, H.S. and H.Y.; methodology, H.S. and S.T.; software, H.S.; validation, H.S., H.Y. and S.T.; formal analysis, H.S.; investigation, H.S.; resources, H.S., H.Y. and S.T.; data curation, H.S.; writing—original draft preparation, H.S.; writing—review and editing, H.Y. and S.T.; visualization, H.S.; supervision, H.Y.; project administration, H.S.; funding acquisition, H.S., H.Y. and S.T. All authors have read and agreed to the published version of the manuscript.

Funding: The work presented in this paper is financially supported by National Natural Science Foundation of China with an account number of 52206248; the Fundamental Research Funds for the Central Universities with an account number of D2220740; the Research Institute for Sustainable Urban Development (RISUD), The Hong Kong Polytechnic University; National Natural Science Foundation of China with an account number of 52207111; China Postdoctoral Science Foundation, No. 2023T160311, the Jiangsu Funding Program for Excellent Postdoctoral Talent with an account number of 2022ZB200, and the Foreign Expert Program with an account number of G2022181028L.

Institutional Review Board Statement: Not applicable.

Informed Consent Statement: Not applicable.

Data Availability Statement: The datasets are available on request.

Conflicts of Interest: The authors declare no conflict of interest.

References

1. Sun, H.; Yang, H.; Gao, X. Investigation into wind turbine wake effect on complex terrain. *Energy* **2023**, *269*, 126767. [CrossRef]
2. Sun, H.; Gao, X.; Yang, H. A review of full-scale wind-field measurements of the wind-turbine wake effect and a measurement of the wake-interaction effect. *Renew. Sustain. Energy Rev.* **2020**, *132*, 110042. [CrossRef]
3. Zhou, M.; Zhou, S.; Zhang, X.; Tian, Y. Influence of Spudcan Penetration on Adjacent Skirted Foundation in Uniform Clay. *J. Geotech. Geoenviron. Eng.* **2023**, *149*, 04023072. [CrossRef]
4. González, J.S.; Rodriguez, A.G.G.; Mora, J.C.; Santos, J.R.; Payan, M.B. Optimization of wind farm turbines layout using an evolutive algorithm. *Renew. Energy* **2010**, *35*, 1671–1681. [CrossRef]
5. Bonanni, A.; Banyai, T.; Conan, B.; Van Beeck, J.; Deconinck, H.; Lacor, C. Wind farm optimization based on CFD model of single wind turbine wake. In Proceedings of the European Wind Energy Conference and Exhibition, Copenhagen, Denmark, 16–19 April 2012; pp. 1–10.
6. Gao, X.; Yang, H.; Lu, L. Study on offshore wind power potential and wind farm optimization in Hong Kong. *Appl. Energy* **2014**, *130*, 519–531. [CrossRef]
7. Wu, Y.-K.; Lee, C.-Y.; Chen, C.-R.; Hsu, K.-W.; Tseng, H.-T. Optimization of the Wind Turbine Layout and Transmission System Planning for a Large-Scale Offshore WindFarm by AI Technology. *IEEE Trans. Ind. Appl.* **2014**, *50*, 2071–2080. [CrossRef]
8. Hou, P.; Hu, W.; Soltani, M.; Chen, Z. Optimized Placement of Wind Turbines in Large-Scale Offshore Wind Farm Using Particle Swarm Optimization Algorithm. *IEEE Trans. Sustain. Energy* **2015**, *6*, 1272–1282. [CrossRef]
9. Kuo, J.Y.; Romero, D.A.; Amon, C.H. A mechanistic semi-empirical wake interaction model for wind farm layout optimization. *Energy* **2015**, *93*, 2157–2165. [CrossRef]
10. Amaral, L.; Castro, R. Offshore wind farm layout optimization regarding wake effects and electrical losses. *Eng. Appl. Artif. Intell.* **2017**, *60*, 26–34. [CrossRef]
11. Ju, X.; Liu, F. Wind farm layout optimization using self-informed genetic algorithm with information guided exploitation. *Appl. Energy* **2019**, *248*, 429–445. [CrossRef]
12. Ju, X.; Liu, F.; Wang, L.; Lee, W.-J. Wind farm layout optimization based on support vector regression guided genetic algorithm with consideration of participation among landowners. *Energy Convers. Manag.* **2019**, *196*, 1267–1281. [CrossRef]
13. Yang, K.; Kwak, G.; Cho, K.; Huh, J. Wind farm layout optimization for wake effect uniformity. *Energy* **2019**, *183*, 983–995. [CrossRef]
14. Gualtieri, G. Comparative analysis and improvement of grid-based wind farm layout optimization. *Energy Convers. Manag.* **2020**, *208*, 112593. [CrossRef]
15. Liu, F.; Ju, X.; Wang, N.; Wang, L.; Lee, W.-J. Wind farm macro-siting optimization with insightful bi-criteria identification and relocation mechanism in genetic algorithm. *Energy Convers. Manag.* **2020**, *217*, 112964. [CrossRef]
16. Chen, Y.; Li, H.; Jin, K.; Song, Q. Wind farm layout optimization using genetic algorithm with different hub height wind turbines. *Energy Convers. Manag.* **2013**, *70*, 56–65. [CrossRef]
17. Mittal, P.; Kulkarni, K.; Mitra, K. A novel hybrid optimization methodology to optimize the total number and placement of wind turbines. *Renew. Energy* **2016**, *86*, 133–147. [CrossRef]

18. Herbert-Acero, J.-F.; Franco-Acevedo, J.-R.; Valenzuela-Rendón, M.; Probst-Oleszewski, O. Linear Wind Farm Layout Optimization through Computational Intelligence. In Proceedings of the Mexican International Conference on Artificial Intelligence, Guanajuato, Mexico, 9–13 November 2009; Springer: Berlin/Heidelberg, Germany, 2009; pp. 692–703.
19. Kusiak, A.; Song, Z. Design of wind farm layout for maximum wind energy capture. *Renew. Energy* **2010**, *35*, 685–694. [CrossRef]
20. Mittal, P.; Mitra, K. Decomposition based multi-objective optimization to simultaneously determine the number and the optimum locations of wind turbines in a wind farm. *IFAC-Pap.* **2017**, *50*, 159–164. [CrossRef]
21. Pérez, B.; Mínguez, R.; Guanche, R. Offshore wind farm layout optimization using mathematical programming techniques. *Renew. Energy* **2013**, *53*, 389–399. [CrossRef]
22. Rodrigues, S.; Pinto, R.T.; Soleimanzadeh, M.; Bosman, P.A.; Bauer, P. Wake losses optimization of offshore wind farms with moveable floating wind turbines. *Energy Convers. Manag.* **2015**, *89*, 933–941. [CrossRef]
23. Hou, P.; Hu, W.; Chen, C.; Soltani, M.; Chen, Z. Optimization of offshore wind farm layout in restricted zones. *Energy* **2016**, *113*, 487–496. [CrossRef]
24. Gebraad, P.; Thomas, J.J.; Ning, A.; Fleming, P.; Dykes, K. Maximization of the annual energy production of wind power plants by optimization of layout and yaw-based wake control. *Wind Energy* **2017**, *20*, 97–107. [CrossRef]
25. Kirchner-Bossi, N.; Porté-Agel, F. Realistic Wind Farm Layout Optimization through Genetic Algorithms Using a Gaussian Wake Model. *Energies* **2018**, *11*, 3268. [CrossRef]
26. Song, M.; Chen, K.; Wang, J. Three-dimensional wind turbine positioning using Gaussian particle swarm optimization with differential evolution. *J. Wind Eng. Ind. Aerodyn.* **2018**, *172*, 317–324. [CrossRef]
27. Reddy, S.R. Wind Farm Layout Optimization (WindFLO): An advanced framework for fast wind farm analysis and optimization. *Appl. Energy* **2020**, *269*, 115090. [CrossRef]
28. Moreno, S.R.; Pierezan, J.; Coelho, L.d.S.; Mariani, V.C. Multi-objective lightning search algorithm applied to wind farm layout optimization. *Energy* **2021**, *216*, 119214. [CrossRef]
29. Mustakerov, I.; Borissova, D. Wind turbines type and number choice using combinatorial optimization. *Renew. Energy* **2010**, *35*, 1887–1894. [CrossRef]
30. Ekonomou, L.; Lazarou, S.; Chatzarakis, G.; Vita, V. Estimation of wind turbines optimal number and produced power in a wind farm using an artificial neural network model. *Simul. Model. Pract. Theory* **2012**, *21*, 21–25. [CrossRef]
31. Feng, J.; Shen, W.Z.; Xu, C. Multi-Objective Random Search Algorithm for Simultaneously Optimizing Wind Farm Layout and Number of Turbines. *J. Physics Conf. Ser.* **2016**, *753*, 032011. [CrossRef]
32. Mittal, P.; Mitra, K.; Kulkarni, K. Optimizing the number and locations of turbines in a wind farm addressing energy-noise trade-off: A hybrid approach. *Energy Convers. Manag.* **2017**, *132*, 147–160. [CrossRef]
33. Vasel-Be-Hagh, A.; Archer, C.L. Wind farm hub height optimization. *Appl. Energy* **2017**, *195*, 905–921. [CrossRef]
34. Mosetti, G.; Poloni, C.; Diviacco, B. Optimization of wind turbine positioning in large windfarms by means of a genetic algorithm. *J. Wind Eng. Ind. Aerodyn.* **1994**, *51*, 105–116. [CrossRef]
35. Sun, H.; Yang, H. Numerical investigation of the average wind speed of a single wind turbine and development of a novel three-dimensional multiple wind turbine wake model. *Renew. Energy* **2020**, *147*, 192–203. [CrossRef]
36. Jensen, N.O. *A Note on Wind Generator Interaction*; Riso National Laboratory, DK-4000: Roskilde, Denmark, 1983.
37. Sun, H.; Qiu, C.; Lu, L.; Gao, X.; Chen, J.; Yang, H. Wind turbine power modelling and optimization using artificial neural network with wind field experimental data. *Appl. Energy* **2020**, *280*, 115880. [CrossRef]
38. Sun, H.; Yang, H.; Gao, X. Investigation into spacing restriction and layout optimization of wind farm with multiple types of wind turbines. *Energy* **2018**, *168*, 637–650. [CrossRef]
39. Sun, H.; Yang, H. Wind farm layout and hub height optimization with a novel wake model. *Appl. Energy* **2023**, *348*, 121554. [CrossRef]
40. Wikipedia. Hong Kong. Available online: https://en.wikipedia.org/wiki/Hong_Kong (accessed on 1 June 2023).
41. Sun, H.; Gao, X.; Yang, H. Investigation into offshore wind farm repowering optimization in Hong Kong. *Int. J. Low-Carbon Technol.* **2019**, *14*, 302–311. [CrossRef]
42. Wikipedia. Wind Profile Power Law. Available online: https://en.wikipedia.org/wiki/Wind_profile_power_law (accessed on 1 June 2023).